

Improvement of precipitation prediction and model output over mountainous regions by using the equivalent geopotential tested in the MM5

Qiu-shi Chen, Lesheng Bai and David H. Bromwich

Polar Meteorology Group, Byrd Polar Research Center, The Ohio State University, Columbus

1 Introduction

Mountains have important influences on large- and mesoscale meteorological phenomena, and one of profound effects is on precipitation. Colle et al. (1999) verified the 36- and 12-km resolution Penn State/NCAR Mesoscale Model (MM5) precipitation forecasts from 9 December 1996 through 30 April 1997 and NCEP's 10-km resolution Eta Model (Eta-10) forecasts from 7 January 1997 through 30 April 1997 across Pacific West. It is found that the 12-km MM5 tends to generate too much precipitation along the steep windward slopes and not enough precipitation in the lee of major barriers. The Eta-10 overpredicts precipitation along the windward slopes even more than the 12-km MM5. Cassano et al. (2001) used the Polar MM5 to simulate a complete annual cycle from April 1997 through March 1998 over the Greenland ice sheet. The modeled precipitation is excessive along the steep coastal margins with spot value in excess of 400 cm/yr located on the southeast coast where has the steepest windward slope while the corresponding observed value is about 120 cm/yr.

As has been understood for decades, the horizontal pressure gradient force (HPGF) in terrain-following (including pressure-based and height-based) coordinates is a small difference between two large terms over steep slopes and its computational errors are very large. This problem also arises in the nonhydrostatic model MM5 formulated in terms of pressure perturbation relative to a hydrostatic reference state. Dempsay and Davis (1998) gave an error analysis of the MM5's HPGF schemes, and found that the standard HPGF scheme in MM5 can produce significant velocity errors above steep terrain. Some alternative schemes may reduce, but cannot eliminate, these errors. Mesinger (1984) developed the step-mountain approach of the Eta-coordinate system to calculate the pressure gradient in a region of complex terrain. However, the piecewise constant representation of the terrain is only first-order accurate in mathematics. Based on Z. Janjic (1998), Colle et al. (1999) pointed out that the Eta-10 produces excessive flow blocking upwind of major barriers and results in too much upward motion and precipitation well upwind of the orographic crest. Furthermore, physical parameterizations in the planetary boundary layer are straightforward with the terrain-following coordinates. At present, many global and limited-area models, for example, the WRF model, still use terrain-following coordinates.

Recently Chen and Bromwich (1999, hereafter referred to as CB99) proposed a new method to compute the HPGF in σ -coordinates and this method uses terrain-following coordinates. The horizontal wind can be separated into its irrotational and rotational parts in a limited region (Chen and Kuo, 1992). The HPGF \mathbf{G} in σ -coordinates is also a

horizontal vector and can also be separated into its irrotational and rotational components in a limited region and expressed by

$$\mathbf{G} = -\nabla\Phi_e - \mathbf{k} \times \nabla\eta \quad (1)$$

where Φ_e and η are referred to as equivalent geopotential and geo-streamfunction, respectively.

In the ordinary σ -coordinates, $\sigma = p/p_*(x,y,t)$, where $p_*(x,y,t)$ is the earth's surface pressure, the HPGF \mathbf{G} of a hydrostatic model can be expressed by

$$\mathbf{G} = -\nabla\Phi(x,y,\sigma,t) - RT\nabla \ln p_*(x,y,t) \quad (2)$$

where $\Phi(x,y,\sigma,t)$ is the geopotential. In this hydrostatic model, the equivalent geopotential Φ_e and geo-streamfunction η in limited region are derived from the corresponding Poisson equations. In a nonhydrostatic model, for examples, the MM5 or WRF, the HPGF has its specific expression, from which the corresponding Poisson equations and boundary conditions can also be derived and solved.

Comparing $\Phi_e(x,y,\sigma,t)$ with $\Phi(x,y,p,t)$, both $-\nabla\Phi_e(x,y,\sigma,t)$ and $-\nabla\Phi(x,y,p,t)$ are the same irrotational part of the HPGF, but they are in p - and σ -coordinates, respectively. The HPGF in p -coordinates, $\nabla\Phi(x,y,p,t)$, has only the irrotational part. The rotational part can only be computed through the lower boundary condition at $p=p_*(x,y,t)$ or $z = H_*(x,y)$ implicitly. In general, the rotational part of the HPGF is much smaller than its irrotational part. It has been shown in Table 1 of CB99 that the absolute value of the rotational part in σ -coordinates is very small comparing to the irrotational part over the Greenland including steep slopes. Thus, although there are two terms in the expression (1) of the HPGF, the small difference between two large terms over steep slopes is eliminated automatically.

Because $-\nabla\Phi(x,y,p,t)$ and $-\nabla\Phi_e(x,y,\sigma,t)$ are the same irrotational part of the HPGF, the equivalent geopotential $\Phi_e(x,y,\sigma,t)$ in σ -coordinates can be used in the same way as $\Phi(x,y,p,t)$ is used in p -coordinates. The equivalent geopotential Φ_e can be used in synoptic analysis on constant σ surface, and several examples of the equivalent geopotential analysis at $\sigma=0.995$ have been shown in CB99. Many artificial anomalous systems over the Tibetan Plateau and Greenland in the sea-level pressure maps caused by pressure reduction to the sea level are all removed in the analyses on the constant σ -surface at $\sigma=0.995$, and the behaviors of weather systems over the surface of high mountain regions are shown clearly in the constant $\sigma=0.995$ surface analyses. The analyses in CB99 show that the geostrophic relation $\Phi_e = f_0\psi$ between the equivalent geopotential and rotational wind is approximately satisfied on the constant σ surface for the synoptic scale motions, and it is the same as that $\Phi = f_0\psi$ on the isobaric surface.

2. The perturbation method and the equations of the equivalent geopotential and geo-streamfunction for the MM5

a. Perturbation method used in the HPGF computation

The pressure in the MM5 in z-coordinates is denoted by $p(x, y, z, t) = p_0(z) + p'(x, y, z, t)$ where $p_0(z)$ and $p'(x, y, z, t)$ are the pressure of a hydrostatic balanced reference state and its perturbation, respectively. In the WRF model, the dynamic equations are different from the MM5's, but a similar perturbation method is also used. Because the hydro balanced reference state is artificially given, the most of p' is the hydrostatic pressure rather than the dynamic pressure if the dynamic pressure is defined as the difference between the pressure and hydrostatic pressure. The vertical coordinate σ in the MM5 is defined by

$$\sigma = \frac{p_0 - p_t}{p_s(x, y) - p_t} = \frac{p_0 - p_t}{p^*}$$

where $p^*(x, y) = p_s(x, y) - p_t$. Here $p_s(x, y)$ is the stationary surface pressure and determined from a given temperature profile and terrain height and p_t is top pressure. The pressure in σ -coordinates is given by

$$p = p_{r0} + p' = p^* \sigma + p_t + p'$$

where $p_{r0}(x, y, \sigma)$ is expressed by

$$p_{r0} = p - p' = p^* \sigma + p_t$$

and $p' = p - p_{r0}$. They are the stationary and non-stationary parts of the pressure in σ -coordinates, respectively.

The x- and y-components of the momentum equations in MM5 are denoted by

$$\frac{\partial(u/m)}{\partial t} + \frac{1}{\rho} \left(\frac{\partial p'}{\partial x} - \frac{\sigma}{p^*} \frac{\partial p'}{\partial x} \right) = F_x \quad (3)$$

$$\frac{\partial(v/m)}{\partial t} + \frac{1}{\rho} \left(\frac{\partial p'}{\partial y} - \frac{\sigma}{p^*} \frac{\partial p'}{\partial y} \right) = F_y \quad (4)$$

where F_x and F_y are advection and other terms. The HPGF in (3) and (4) is expressed by

$$\mathbf{G} = -\frac{1}{\rho} \left(\nabla p' - \frac{\sigma}{p^*} \frac{\partial p'}{\partial \sigma} \nabla p^* \right) = -\frac{1}{\rho} (\nabla p' - \tau \nabla p_{r0}) \quad (1a)$$

where
$$\tau = \frac{1}{p^*} \frac{\partial p'}{\partial \sigma} = \left(\frac{\partial p_{r0}}{\partial \sigma} \right)^{-1} \frac{\partial p'}{\partial \sigma}$$

Now we use the distribution of $p'(x, y, \sigma, t)$ on the constant σ surfaces to check qualitatively whether or not the sum of the two terms on the right hand side of (1a) over steep slopes is a small difference between two large terms. If so, the gradient of p' must be extremely large over steep slopes. In p-coordinates, the distribution of geopotential is closely related to distribution of synoptic and mesoscale weather systems and has no relation to the topography even over very steep slopes. In the σ -coordinates, the distribution of $\Phi(x, y, \sigma, t)$ or $\ln p^*(x, y, t)$ represent not only the features of the weather systems but also the effects from topography. The steeper the slopes are, the larger the horizontal gradient of Φ and or $\ln p^*$ become. Thus, the gradient of Φ is extremely large over steep slopes. This characteristic on the constant σ surfaces can also be used to study the two terms on the right hand side of (1a). Figures 1(a) and 1(b) show the distribution of $p'(x, y, \sigma, t)$ on the constant $\sigma = 0.9975$ surface at 0000 UTC 26 and at 1200 UTC 27 January 1999, respectively. In Fig. 1(a), most of the topographic effects are removed,

and the horizontal gradient of p' is not very large over steep slopes. However, after 36 hours, the horizontal gradient of p' is particularly large along the east coast of Greenland. At this time, the computation of the HPGF must have large errors based on the two terms on the right hand side of (1a) in this coastal region. This is because the separation method uses a given temperature profile $T_0(p)$. If the deviation $T - T_0(p)$ is very small, the perturbation method may reduce some computation errors of the HPGF over mountainous regions. If the deviation $T - T_0(p)$ is very large over steep slopes, the computation of the HPGF is still a small difference between two large terms on the right hand side of (1a) in this region. The above results state that the method of separating the HPGF into a hydrostatic balanced reference state and its perturbation in terrain-following coordinates cannot guarantee to reduce errors of the HPGF computation over steep slopes. However, if the equivalent geopotential and geo-streamfunction are used in the computation of the HPGF, no any $T_0(p)$ is used. The figure 1(c) shows the distribution of the equivalent geopotential, (of which the computation method is shown in the following subsection), at the same time of Fig. 1(b). It is seen that the Φ_e is very smooth over steep slopes. The errors of the HPGF computation can be solved completely by using the Φ_e .

b. The equations of the inner and harmonic parts of the equivalent geopotential and geo-streamfunction for the HPGF of the MM5

If the HPGF (1a) is separated into the rotational and irrotational parts, the equivalent geopotential Φ_e and the geo-streamfunction η satisfy the Poisson equations

$$\nabla^2 \Phi_e = \frac{\partial}{\partial x} \left(\frac{1}{\rho} \frac{\partial p'}{\partial x} \right) + \frac{\partial}{\partial y} \left(\frac{1}{\rho} \frac{\partial p'}{\partial y} \right) - \left\{ \frac{\partial}{\partial x} \left(\frac{\tau}{\rho} \frac{\partial p_{r0}}{\partial x} \right) + \frac{\partial}{\partial y} \left(\frac{\tau}{\rho} \frac{\partial p_{r0}}{\partial y} \right) \right\} \quad (5)$$

$$\nabla^2 \eta = \frac{\partial}{\partial x} \left(\frac{1}{\rho} \right) \frac{\partial p'}{\partial y} - \frac{\partial}{\partial y} \left(\frac{1}{\rho} \right) \frac{\partial p'}{\partial x} - \left\{ \frac{\partial}{\partial x} \left(\frac{\tau}{\rho} \frac{\partial p_{r0}}{\partial y} \right) + \frac{\partial}{\partial y} \left(\frac{\tau}{\rho} \frac{\partial p_{r0}}{\partial x} \right) \right\} \quad (6)$$

Over the globe, the above Poisson equations are easily solved without lateral boundary conditions. If they are solved in a limited region, the boundary condition is expressed by

$$\mathbf{s} \cdot \mathbf{G} = \frac{\partial \eta}{\partial n} + \frac{\partial \Phi_e}{\partial s} = G_t = -\frac{1}{\rho} \frac{\partial p'}{\partial s} + \frac{\tau}{\rho} \frac{\partial p_{r0}}{\partial s} \quad (7)$$

$$\mathbf{n} \cdot \mathbf{G} = -\frac{\partial \eta}{\partial s} + \frac{\partial \Phi_e}{\partial n} = G_n = -\frac{1}{\rho} \frac{\partial p'}{\partial n} + \frac{\tau}{\rho} \frac{\partial p_{r0}}{\partial n} \quad (8)$$

where \mathbf{s} and \mathbf{n} are tangential and normal unit vectors, respectively, and s and n are distances along and normal to the boundary. In this case, the equivalent geopotential and geo-streamfunction are derived by solving Poisson equations (5) and (6) with the coupled boundary conditions (7) and (8).

Using the harmonic-sine series, the solutions for Φ_e and η can be separated into their inner and harmonic parts as

$$\Phi_e = \Phi_{ei} + \Phi_{eh}, \quad \eta = \eta_i + \eta_h \quad (9)$$

where Φ_{eh} , η_h and Φ_{ei} , η_i are the harmonic and inner parts of the equivalent geopotential and the geo-streamfunction, respectively. The inner parts, Φ_{ei} and η_i , satisfy Poisson equations (5) and (6) with zero Dirichlet boundary value. The solutions for Φ_{ei} and η_i can be easily

derived by using a double Fourier sine series. The internal HPGF is then computed by

$$G_{xi} = -\frac{\partial \eta_i}{\partial y} + \frac{\partial \phi_{ei}}{\partial x}, \quad G_{yi} = \frac{\partial \eta_i}{\partial x} + \frac{\partial \phi_{ei}}{\partial y} \quad (10)$$

where G_{xi} and G_{yi} are the components of the internal HPGF. In a limited region, the difference between the HPGF and internal HPGF is denoted by

$$G_{xE} = G_x - G_{xi} = -\frac{1}{\rho} \frac{\partial p'}{\partial x} + \frac{\tau}{\rho} \frac{\partial p_{r0}}{\partial x} - G_{xi} \quad (11)$$

$$G_{yE} = G_y - G_{yi} = -\frac{1}{\rho} \frac{\partial p'}{\partial y} + \frac{\tau}{\rho} \frac{\partial p_{r0}}{\partial y} - G_{yi} \quad (12)$$

and G_{xE} and G_{yE} are referred to as the components of the external HPGF. Utilizing (1), (9) and (10), the external HPGF can be expressed by the harmonic parts of the equivalent geopotential and the geo-streamfunction as

$$G_{xE} = -\frac{\partial \eta_h}{\partial y} + \frac{\partial \phi_h}{\partial x}, \quad G_{yE} = \frac{\partial \eta_h}{\partial x} + \frac{\partial \phi_h}{\partial y} \quad (13)$$

The harmonic parts of the equivalent geopotential and the geo-streamfunction satisfy the Laplace equations

$$\nabla^2 \phi_{eh} = 0, \quad \nabla^2 \eta_h = 0 \quad (14)$$

Thus, the external HPGF is not only non-divergent but also irrotational in a limited region. The coupled boundary conditions (7) and (8) for solving Laplace equations (14) of the harmonic parts in region R become

$$\frac{\partial \eta_h}{\partial n} + \frac{\partial \phi_{eh}}{\partial s} = G_{Et} = -\frac{1}{\rho} \frac{\partial p'}{\partial s} + \frac{\tau}{\rho} \frac{\partial p_{r0}}{\partial s} - G_{hi} \quad (15)$$

$$-\frac{\partial \eta_h}{\partial s} + \frac{\partial \phi_{eh}}{\partial n} = G_{En} = -\frac{1}{\rho} \frac{\partial p'}{\partial n} + \frac{\tau}{\rho} \frac{\partial p_{r0}}{\partial n} - G_{in} \quad (16)$$

where G_{Et} and G_{En} are the tangential and normal components of the external HPGF at the boundary.

3 Precipitation over Greenland modeled by the MM5 with Φ_e

Now we will show a synoptic example, in which there is a cyclone moving across the southern part of Greenland. The southeast coast is in the windward slopes, while the west coast of the central and southern parts is in the lee side. The 36 hr predictions of the sea-level pressure (SLP) and Φ_{ei} at $\sigma=0.9975$ (at 1200 UTC 27 January 1999) by the models with Φ_e are given in Figs. 2a and 2b, respectively. It is seen that the weather systems over Greenland are shown more clearly and smoothly on the constant σ -surfaces than the SLP maps. The 36 hr predictions of the precipitation by the models without and with Φ_e are given (omitted) and their distribution patterns look like the same. Figure 2c shows the difference of the 36 hr precipitation prediction by the models with and without Φ_e , $P(\text{with } \Phi_e) - P(\text{without } \Phi_e)$. It is seen from Fig. 2c that the negative areas are located primarily in the windward slopes of the southeast coast of Greenland. It means that the modeled precipitation with Φ_e decreases in the windward slopes. The positive areas are primarily located in the lee side of the west coast of the central and southern parts. The modeled precipitation with Φ_e

increases in this region. Thus, Fig. 2c shows that the precipitation prediction errors of the MM5 found by Colle et al. (1999) and Cassano et al. (2001) can be reduced by using Φ_e in the model without any other changes.

4. Conclusion

(1) The HPGF in σ -coordinates can be separated into its rotational and irrotational parts, expressed by the equivalent geopotential and geo-streamfunction, respectively. This separation method can be used in the HPGF computation in a dynamic model and has the important physical basis. The Φ_e is computed from time dependent $T(x,y,\sigma,t)$, while p' is computed from a given $T_0(p)$. The Φ_e is always very smooth over steep slopes but p' cannot. Thus, the equivalent geopotential is much better than p' .

(2) If this method is used in the MM5 instead of its original HPGF scheme over Greenland, the simulated precipitation by the model with Φ_e decreases in the windward slopes of the southeast coast, but increases in lee side. This method can improve the precipitation prediction of the MM5 near the steep slopes.

(3) The equivalent geopotential can be used in synoptic analysis and model outputs directly on constant σ -surfaces, and it is in the same way as $\Phi(x, y, p, t)$ is used in p -coordinates. The model outputs are not necessary to be transferred to p -coordinates and they can be examined directly in σ -coordinates. By this method, weather systems over high mountain regions can be shown clearly and correctly on the constant σ -surfaces near the earth's surface.

Reference

- Cassano, J. J., J. E. Box, D. H. Bromwich, L. Li, and K. Steffen, 2001: Verification of polar MM5 simulations of Greenland's atmospheric circulation. *J. Geophys. Res.*, **106**(D24), 33,867-33,890.
- Chen, Q.-S., and Y.-H. Kuo, 1992: A harmonic-sine series expansion and its application to the partitioning and reconstruction problem in a limited area. *Mon. Wea. Rev.*, **120**, 91-112.
- Chen, Q.-S., and D. H. Bromwich, 1999: An equivalent isobaric geopotential height and its application to synoptic analysis and to a generalized ω -equation in σ -coordinates. *Mon. Wea. Rev.*, **127**, 145-172.
- Colle B. A., K. J. Westrick, and C. F. Mass, 1999: Evaluation of MM5 and Eta-10 precipitation forecasts over the Pacific Northwest during the cool season. *Weather and Forecasting*, **14**, 137-154.
- Dempsey, D. and C. Davis, 1998: Error analyses and test of pressure gradient force schemes in nonhydrostatic, mesoscale model. *Preprints, 12th Conf. on Numerical Weather Prediction*, 11-16 January 1998, Phoenix, AZ, Amer. Meteor. Soc., 236-239.
- Mesinger, F., 1984: A blocking technique for representation of mountains in atmospheric models. *Rev. Meteorol. Aeronautica.*, **44**, 195-202.

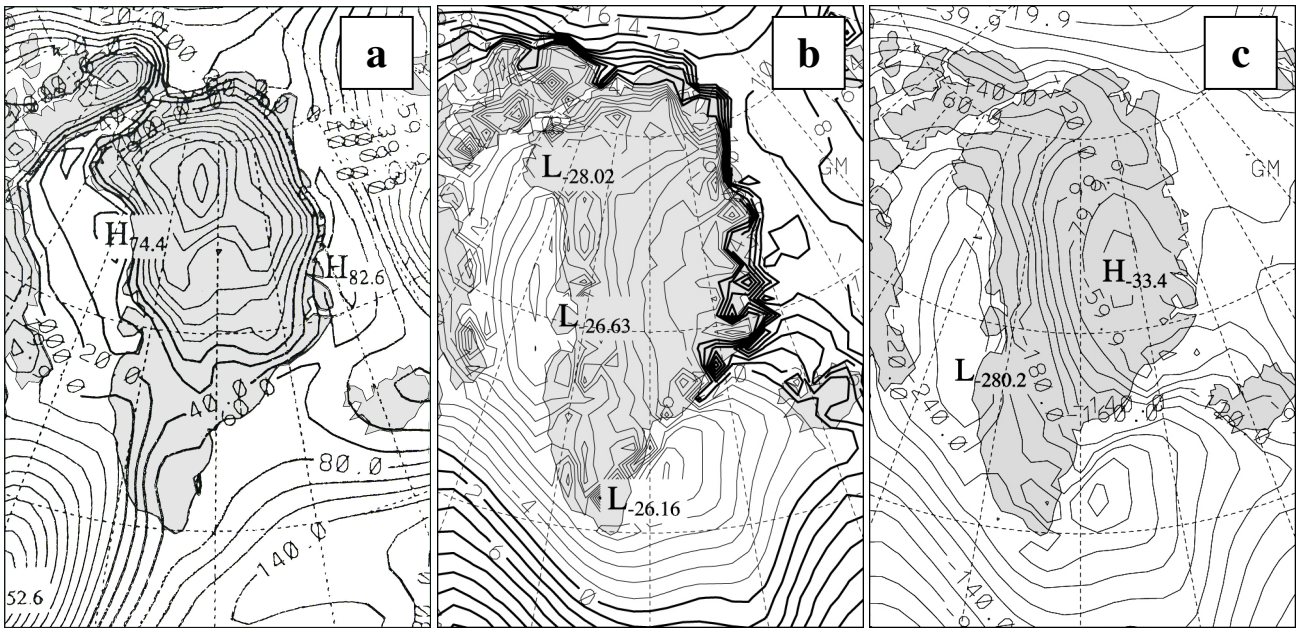


Fig.1 a. The pressure perturbation p' at 0000 UTC 26 January 1999 at $\sigma=0.9975$ (90 km grid length). b. The pressure perturbation p' at 1200 UTC 27 January 1999 at $\sigma=0.9975$ (90 km grid length). c. The inner part of the equivalent geopotential at 1200 UTC 27 January 1999 at $\sigma=0.9975$.

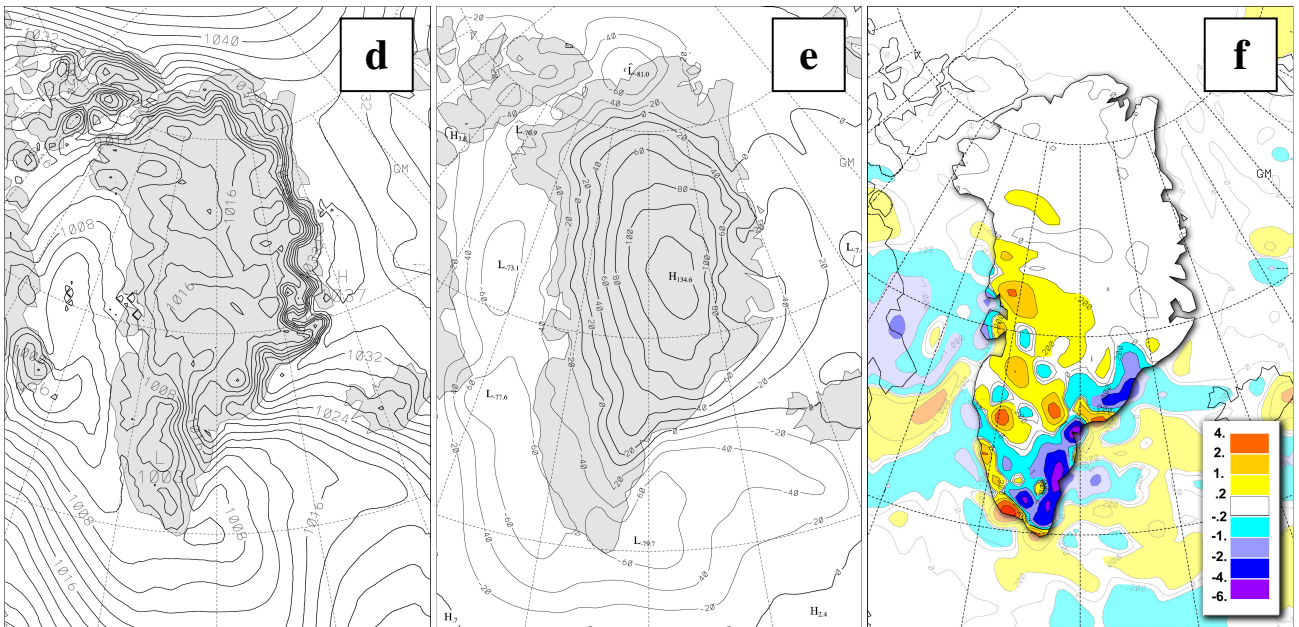


Fig.2 a. The 36hr prediction of sea level pressure (at 1200 UTC January 1999) by the model with ϕ_e . b. The equivalent geopotential at 0000 UTC 27 January 1999 at $\sigma=0.9975$. c. The difference of the 36hr precipitation prediction by the models with ϕ_e and without ϕ_e , i.e., $P(\text{with } \phi_e) - P(\text{without } \phi_e)$.